https://doi.org/10.5194/acp-2021-454
Preprint. Discussion started: 5 July 2021

Atmospheric Chemistry and Physics Discussions

Characterizing the volatility and mixing state of ambient fine particles in summer and winter of urban Beijing

Lu Chen[1], Fang Zhang[1*], Don Collins[2], Jieyao Liu[1], Sihui Jiang[1], Jingye Ren[1], Zhanqing Li[3]

[1]College of Global Change and Earth System Science, Beijing Normal University, Beijing 100875, China
[2]Chemical and Environmental Engineering, University of California, Riverside, CA 92521, USA
[3]Earth System Science Interdisciplinary Center and Department of Atmospheric and Oceanic Science, University of Maryland, College Park, MD, USA

Correspondence to: F. Zhang (*fang.zhang@bnu.edu.cn*)

Abstract. Understanding the volatility and mixing state of atmospheric aerosols is important for elucidating the formation of fine particles and to help determining their effect on environment and climate. In this study, the volatility of the fine particles is characterized by the size-dependent volatility shrink factor (VSF) for summer and winter in the urban area of Beijing using measurements of a volatility tandem differential mobility analyzer (VTDMA). We show the volatility of aerosols is always with one high-volatile and one less- or non-volatile mode both in the summer and winter. On average, the particles are more volatile in the summer (with mean VSF of 0.3) than in the winter (with mean VSF of 0.6). The outstanding high-volatile mode around noontime illustrates the role of nucleation in producing more volatile particles in the summer. We further retrieve the mixing state of the ambient fine particles from the size-resolved VSF and find that the non-black carbon (BC) particles that formed from nucleation processes accounted for 52–69 % of the total number concentration in the summer. While, particles containing a refractory core that is thought to be BC-containing particles dominate and contribute 67–77 % toward the total number concentration in the winter. The diurnal cycles of the retrieved aerosol mixing state for the summer further supports the conclusion that nucleation process is the main contributors to non-BC particles. In addition, the extent of aging of BC particles was characterized as the ratio of the BC diameter before and after heating at 300 ℃ (D_p/D_c), showing that the average ratio of ~2.2 in the winter is higher than the average of ~1.5 in the summer, which indicates that BC aging is more efficient in wintertime, with resulting differences in light absorption enhancement between cold and warm seasons.

https://doi.org/10.5194/acp-2021-454
Preprint. Discussion started: 5 July 2021


Atmospheric Chemistry and Physics Discussions

1 Introduction

The volatility of atmospheric aerosols affects their effect on climate, visibility and human health (Dzubay et al., 1982; Pöschl, 2005; Baklanov et al., 2016) by modulating mass concentrations and size distributions of aerosol particles via gas-particle partitioning. Aerosol measurement could be largely biased under different temperatures because of volatility (Meyer et al., 2000; Grieshop et al., 2006; Chen et al., 2010). In addition, volatility influences the partitioning of aerosols in gas and particle phases, and thus affects dry and wet deposition rates (Bidleman, 1988), chemical reaction mechanisms, and atmospheric lifetime (Huffman et al., 2009; Glasius and Goldstein, 2016). Therefore, it is important to study the volatility of aerosols in different regions and environments, including in polluted urban areas.

Laboratory and field measurements have shown that aerosol volatility is correlated with chemical composition of the particles, which is impacted by emission sources and atmospheric processes (Wehner et al., 2004; Yeung et al., 2014). Therefore, the volatility of fine particles varies greatly with time and location. A common measure of volatility is the shrink factor (VSF, the ratio of the particle diameter after and before being heated), which is measured by volatility tandem differential mobility analyzer (VTDMA). The VSF can range from as low as 0 (completely volatile compounds) to 1 (indicating completely non-volatile substances, e.g. black carbon), reflecting heterogeneity in particle composition in diverse environments (Wang et al., 2017; Chen et al., 2020). In addition, the dependence of particle volatility on particle size is complex. For example, Wang et al. (2017) found that ambient aerosol volatility typically decreases as particle size increases in urban Beijing, whereas Levy et al. (2014) showed the opposite dependence on size near the California-Mexico border. Numerous studies have linked aerosol volatility to the presence and abundance of refractory carbonaceous compounds by inferring aerosol mixing state and the degree of aging from measured volatility (Wehner et al., 2009; Cheung et al., 2016; Zhang et al., 2016; Zhang et al., 2017; Chen et al., 2020). Mixing state has been found to vary significantly between clean and heavily polluted days (Wehner et al., 2009), with a corresponding decrease in the fraction of externally mixed black carbon (BC) particles from 37 % during clean to 18 % during heavily polluted periods. Cai et al. (2017) showed that nearly all particles partially volatilized at about 300 ℃ in Okinawa, while 15–21 % did not in Pearl River Delta. Saha et al.

https://doi.org/10.5194/acp-2021-454
Preprint. Discussion started: 5 July 2021


Atmospheric Chemistry and Physics Discussions

(2018) found the non-volatile fraction in roadside aerosols was mostly externally mixed. The results from these studies show that aerosol mixing state and degree of aging may differ greatly under diverse ambient conditions. Considering current uncertainties in assessing the radiative forcing of BC particles, which are largely due to uncertainties in the model treatment of BC mixing state, emissions, and removal processes (Cappa et al., 2012; Nordmann et al., 2014), an improved understanding of aerosol volatility and mixing state is hence needed.

Most previous studies in north China have focused on aerosol chemistry, sources, and transport (Wang et al., 2010; Gao et al., 2011; Sun et al., 2016b), but few have linked the volatility and mixing state of the aerosol to its sources, formation and growth. In north China, severe haze usually occurs in the winter season, with extremely high $PM_{2.5}$, while in the summer it occurs much less frequently and with much lower $PM_{2.5}$, with the contrast resulting from influences of multiple factors such as regional and local emissions, particle formation, meteorology, and photochemistry. A comprehensive study on investigating the aerosols volatility and mixing state in different seasons may help to elucidate the fine particles formation mechanisms.

In this study, a VTDMA system (Sakurai et al., 2003; Wehner et al., 2009; Cheung et al., 2016; Wang et al., 2017) was extensively employed in field observations to measure size-resolved volatility at different heating temperatures during wintertime and summertime in Beijing. At the maximum employed heating temperature of 300 ℃, volatile components tend to evaporate while leaving refractory materials such as black carbon (Cheng et al., 2009). Therefore, the VTDMA is also used to determine the mixing state of refractory carbonaceous particles (Wehner et al., 2009; Zhang et al., 2016; Chen et al., 2020). Here, we used the size-dependent VSF as a parameter to quantify the volatility behaviour of fine particles in cold and warm seasons of urban Beijing; the mixing state of ambient fine particles, which is retrieved from size-resolved VSF, in the two seasons is investigated; the seasonal contrast in the degree of aging of the aerosol, characterized by the coating thickness on BC, is also discussed to elucidate the effects of particle growth mechanisms on volatility and mixing state.

https://doi.org/10.5194/acp-2021-454
Preprint. Discussion started: 5 July 2021

2 Materials and Methods

2.1 Sampling site

We conducted two field campaigns from 28 January to 22 February 2019 and 15 July to 7 August 2019 at a site (Nanjiao; 39.81 °N, 116.48 °E) located southeast of urban Beijing. The sampling site is a basic meteorological observation station of the China Meteorological Administration (CMA), which hosts the most comprehensive meteorological observation instruments of all the CMA sites (Fig. 1). The main instruments used in this study were all placed here, which were set up and deployed in a container for measuring the physicochemical properties of aerosol particles simultaneously. The Fifth-ring beltway is nearby the sampling site with no major industrial pollution sources nearby.

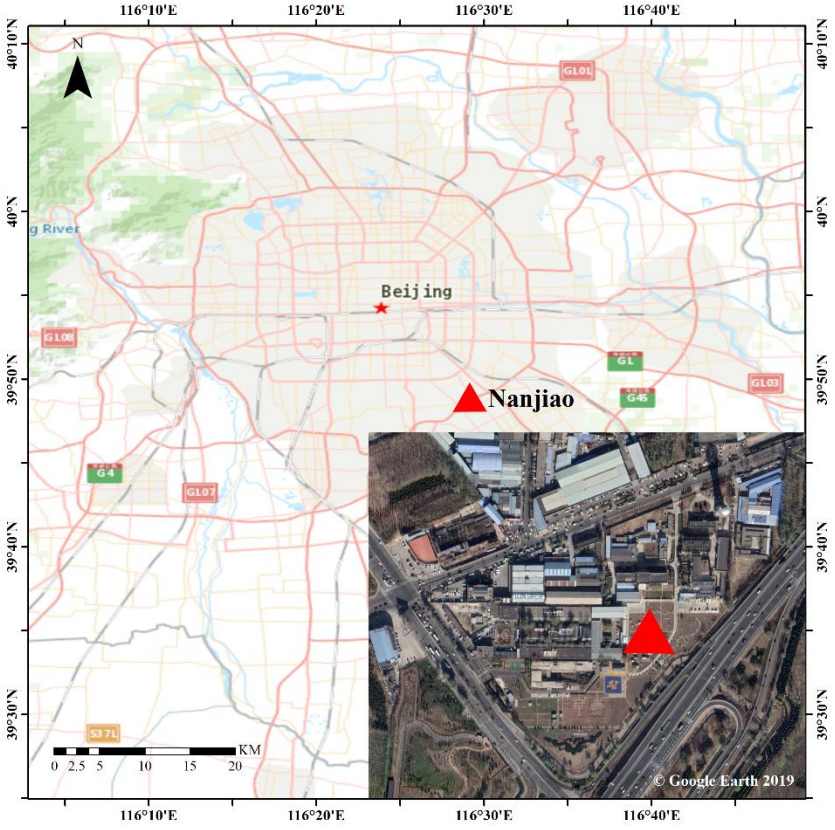

Figure 1. The map of the area surrounding the sampling site (Nanjiao) and true colour image of the observation station. This map was made by ArcGIS (http://www.arcgis.com/index.html#). The true colour image of the observation station was from © Google Earth 2019.

https://doi.org/10.5194/acp-2021-454
Preprint. Discussion started: 5 July 2021


Atmospheric Chemistry and Physics Discussions

2.2 Instruments and measurements

The volatility and mixing state of fine particles were measured with a VTDMA (Fig. S1). Wang et al. (2017) provided a brief description of the custom-made VTDMA system. Here, we give more details. The instrument mainly consists of the following seven parts: neutralizer, the first differential mobility analyzer (DMA_1), temperature control module, the second DMA (DMA_2), water-based condensation particle counter (WCPC, TSI model 3787), auxiliary components (electric steering valve, vacuum pump, proportional valve, etc.), and software for control and data acquisition. During the measurement, ambient aerosols were first sampled by a $PM_{2.5}$ inlet and subsequently passed through a Nafion dryer that reduced the sample flow relative humidity to below 30 %. The dried aerosols were then directed through a neutralizer to neutralize the charge carried by the particles and entered the DMA_1 to produce quasi-monodisperse aerosols by setting the voltage. The dry diameters (D_p) selected in this study were 40, 80, 110, 150, 200 and 300 nm respectively. The selected quasi-monodisperse particles went either to the WCPC to obtain particle counts or through the heating tube for volatility measurements, sequentially at 80, 150, 200 and 300 ℃. Here, we focus on the data derived at 300 ℃. After heating, the sample flow entered the DMA_2 to scan the multi-dispersed particles, and finally entered the WCPC to get the particle size distributions after heating, thereby obtaining the volatility shrink factor measured distribution function (VSF-MDF). Through inversion, the volatility shrink factor probability distribution function (VSF-PDF) could be further obtained. The VSF-PDF was retrieved based on the $TDMA_{inv}$ algorithm developed by Gysel et al. (2009). The residence time in the heated region was 2.4 s (Cheung et al., 2016). Compared with that of 0.3 to 1.5 s for other VTDMA systems (e.g., Brooks et al., 2002; Philippin et al., 2004; Villani et al., 2007; Jiang et al., 2018), the residence time in this VTDMA is sufficient for the volatile materials to be effectively vaporized. The relative humidity was calibrated periodically with ammonium sulfate during the measurement period. Because this study investigates only the fine mode particles below 300 nm, refractory components that are present mostly in coarse mode particles, e.g. dust and sea salt, are expected to be negligible. At around 300–350 ℃, the refractory component in sub micrometer aerosols in continental and urban areas has been considered to be mainly BC and a small contribution by charred organic material, which is often negligible (Rose et al., 2006; Frey et al., 2008; Wehner et al., 2009). For this analysis, BC is assumed to remain in the

https://doi.org/10.5194/acp-2021-454
Preprint. Discussion started: 5 July 2021


Atmospheric Chemistry and Physics Discussions

particle phase upon heating to 300 ℃, while the rest of the aerosol components tend to evaporate, resulting in a reduction in particle size (Cheng et al., 2009).

In addition to the volatility system, some other auxiliary instruments were used for simultaneous observation, including an aerosol chemical speciation monitor (ACSM) for measuring non-refractory submicron aerosols in $PM_{2.5}$, an aethalometer (AE33, Magee Scientific) for measuring the mass concentration of BC, and a scanning mobility particle sizer (SMPS) for measuring the particle number size distribution (PNSD) of aerosols. Before the field measurement, all instruments used were calibrated to ensure the data obtained during the study period were accurate and reliable. The meteorological variables from the meteorological observation station were also used, including the ambient temperature (T), relative humidity (RH), wind direction (WD), and wind speed (WS).

2.3 Data analysis method

In this study, we use the abbreviations Ex-BC, In-BC, and Non-BC to denote externally mixed, internally mixed, and non-BC-containing particles, respectively. The number fraction (Φ_{CV}) of the completely volatile particles was obtained by considering the number concentrations of the residual particles after heating (N_r) and the number concentrations of DMA_1-selected particles before heating (N_{D_p}):

$$\Phi_{CV} = 1 - \frac{N_r}{N_{D_p} \cdot \eta_{D_p,T}} \quad (1)$$

Where $\eta_{D_p,T}$ is the transportation efficiency of the sampled particles, which represents particle losses between DMA_1 and DMA_2 due to diffusion and thermophoretic forces (Philippin et al., 2004), and varies as a function of particle size and heating temperature. In this study, $\eta_{D_p,T}$ at each particle size is determined from the previous experiment results at 300 ℃ (Cheung et al., 2016). The quantified number fraction of completely vaporized particles is shown in Figs. S2 and S3. We then classified the particles into three categories according to the measured VSF values (Wehner et al., 2009; Cheng et al., 2012):

- less-volatile (LV): VSF ≥ 0.82, considered to be Ex-BC;
- medium-volatile (MV): 0.45 ≤ VSF < 0.82, considered to be In-BC;

https://doi.org/10.5194/acp-2021-454
Preprint. Discussion started: 5 July 2021


Atmospheric Chemistry and Physics Discussions

- high-volatile (HV): VSF < 0.45, considered to be Non-BC.

The VSF-PDF ($c(VSF, D_p)$) was normalized as $\int c(VSF, D_p)dVSF = 1$. Then, the number fraction (Φ_i) for each volatile group with the boundary of [VSF_{start}, VSF_{end}] is defined as:

$$\Phi_i = \left[\int_{VSF_{start}}^{VSF_{end}} c(VSF, D_p)dVSF\right] \cdot (1 - \Phi_{CV}) \quad (2)$$

Where i = Ex-BC, In-BC or Non-BC. It is worth noted that, when i = Non-BC, those particles that completely evaporate were assumed to be included in the HV mode (considered as Non-BC), so Φ_{Non-BC} is calculated as:

$$\Phi_{Non-BC} = \left[\int_{VSF_{start}}^{VSF_{end}} c(VSF, D_p)dVSF\right] \cdot (1 - \Phi_{CV}) + \Phi_{CV} \quad (3)$$

The number concentrations (N_i) of In-BC, Ex-BC, and Non-BC from the VSF distributions combined with the total PNSD simultaneously measured by the VTDMA, are calculated as follows:

$$N_i = \Phi_i \cdot N_{total} \quad (4)$$

Here, N_{total} is the number concentrations of ambient fine aerosol particles. Therefore, the actual number fractions of Ex-BC, In-BC and Non-BC particles before heating could be obtained. The retrieval result, which has been compared with the measurements by single particle aerosol mass spectrometer (SPAMS) in previous study (Chen et al., 2020), is reliable for deriving the mixing state of BC.

3 Results and discussion

3.1 Time series of the VSF-PDF

Figure 2 shows the time series of the meteorological parameters, $PM_{2.5}$ concentration, and the VSF-PDF during the winter and summer campaign periods. The T and RH display diurnal cycles. The average T and RH are 0.3 ℃ and 35 % during the winter and 28.3 ℃ and 69 % during the summer. The dominant winds at the site are from the north in the winter and from the south in the summer. The wind speed during the two field campaigns ranged from 2 to about 6 m s^{-1}. More polluted episodes with $PM_{2.5}$ concentration of > 200 μg m^{-3} were more frequent in the winter than in the summer, when the

https://doi.org/10.5194/acp-2021-454
Preprint. Discussion started: 5 July 2021

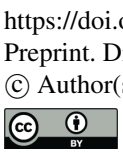

Atmospheric Chemistry and Physics Discussions

$PM_{2.5}$ concentration was < 100 μg m^{-3} on most of the observed days. Figures 2d and 2e display time series of measured VSF-PDF for DMA_1-selected particle sizes of 40 and 150 nm during the two periods. In the summer, the VSF distributions of 40-nm particles were almost always bimodal, with a non-
175 volatile mode (the VSF was approximately equal to 1) and a high volatile mode (with VSF of about 0.2-0.5). As stated above, we attribute the non-volatile group to refractory BC particles. In the winter, the VSF-PDF was bimodal only occasionally, and mostly on polluted days, which could be caused by changes in meteorology and enhanced primary BC emissions during polluted days in the winter. For the 150-nm particles, the distributions are generally unimodal, with VSF of about 0.3-0.6 both in the
180 summer and winter, likely resulting from mixing and aging of the primary particles during growth to larger sizes. The VSF in the summer fluctuated a bit less than that observed in the winter, which will be further discussed in the following section.

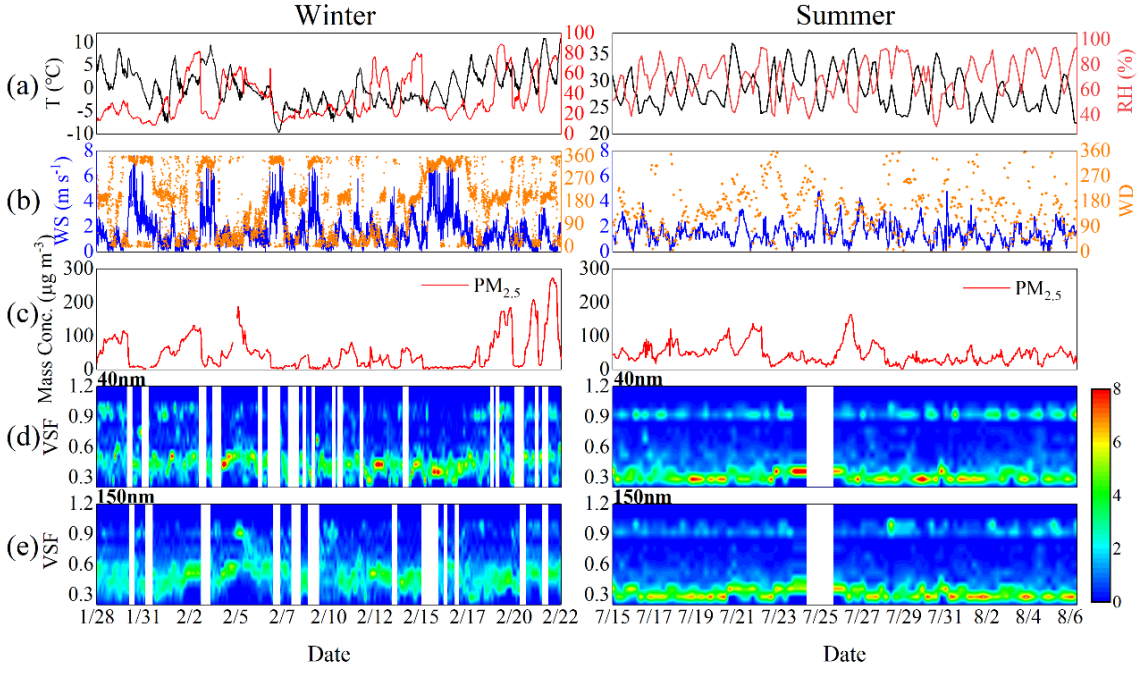

Figure 2. Time series of **(a)** ambient temperature (T) and relative humidity (RH); **(b)** wind direction and wind
185 speed; **(c)** mass concentration of $PM_{2.5}$; **(d-e)** volatility shrink factor distributions (VSF-PDF) for 40- and 150-nm particles at T = 300 °C during the winter (left) and summer (right) periods.

https://doi.org/10.5194/acp-2021-454
Preprint. Discussion started: 5 July 2021


Atmospheric Chemistry and Physics Discussions

3.2 Comparison of the VSF-PDF between summer and winter

Comparison of the average VSF-PDF distribution for all measured dry particle sizes during the winter and summer period is illustrated in Fig. 3. The mean VSF-PDFs are bimodal, with one high-volatile and one less- or non-volatile mode both in the summer and winter. But the mean VSF-PDFs possess an HV mode in the summer, generally with peak values of ~0.2, while an MV mode is present across the size range in the winter (with peak values of 0.45-0.65), indicating higher volatility of the aerosol particles in the summer. In addition, the modes in the VSF-PDFs for the different dry sizes are much broader in the winter than in the summer, reflecting greater heterogeneity in chemical composition.

Our results from Beijing are consistent with those reported previously for other urban environments, with Kuhn et al. (2005), Cheung et al. (2016), Cai et al. (2017), and Jiang et al. (2018) reporting that the VSF-PDFs of fine particles normally has both LV and HV/MV modes. The LV mode consists of non-volatile particles, like BC, the MV mode is comprised of a mixture of volatile (e.g., organics) and non-volatile matter, and the HV mode generally consists of volatile materials that tend to evaporate when heated. In this study, the prominent MV mode in the winter suggests the dominant pathway for fine particle growth is coagulation and condensation of more volatile species (organics or inorganic salts) on non-volatile primary particles (e.g. BC), while the HV mode in the summer may reflect growth of particles that formed from nucleation and grew through addition of volatile organics or inorganic salts.

https://doi.org/10.5194/acp-2021-454
Preprint. Discussion started: 5 July 2021

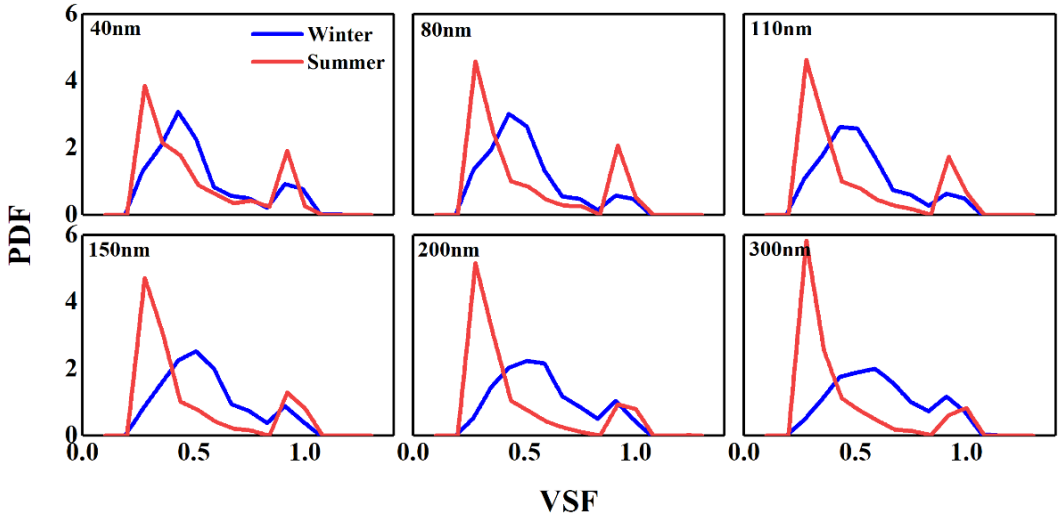

Figure 3. Average volatility shrink factor (VSF) distributions for different sizes (40-300 nm) during the winter (in blue) and summer (in red) observations.

3.3 Comparison of diurnal variation of particles volatility between summer and winter

To obtain further insights into the effect of the formation and growth of particles on their volatility, we compare the diurnal variations of the observed mean VSF and VSF-PDF between the summer and winter (Fig. 4). During the summer, low VSF during the daytime (08:00–18:00 LT) and high VSF during the nighttime were observed (Fig. 4a). Accordingly, the VSF-PDF shows the HV mode dominated around noontime and early afternoon and the LV mode dominated during nighttime (Figs. 4c and 4e). The diurnal variation is more evident for small particles (e.g. 40 nm) than for larger particles (e.g. 150 nm). The diurnal variations illustrate that particles are more volatile during the daytime than at night, with VSF decreasing dramatically after ~10:00 LT when new particle formation (NPF) events usually occurred (Fig. 4g). It has been shown that ~97 % of newly formed particles are volatile because they are dominated by non-refractory sulfate and organics (Wehner et al., 2009). In addition, during daytime atmospheric aging processes facilitated the mixing of primary particles (e.g. BC) with secondary species, leading to the transformation of externally mixed particles to internally mixed particles. In the evening and the early morning, the number fraction of LV-mode particles increased because of increased emissions of refractory particles (like BC) from traffic and other primary sources,

https://doi.org/10.5194/acp-2021-454
Preprint. Discussion started: 5 July 2021

Atmospheric Chemistry and Physics Discussions

coupled with slower particle aging and weaker vertical mixing that concentrates the externally mixed BC close to the surface (Zhang et al., 2016).

Compared with that in the summer, there was little diurnal variation in VSF during the winter period (Fig. 4b), and an MV mode was present in the VSF-PDFs for both 40- and 150-nm particles during the daytime (Figs. 4d and 4f). This is likely because of weakened photochemistry during the daytime in the cold season, when fewer NPF events were observed (Fig. 4h). In addition, the number fraction of the LV mode for both 40- and 150-nm particles is much lower during the winter. This may reflect the fact that BC particles can be coated and aged quickly through heterogeneous reactions of VOCs and other precursor gases (like SO_2 and NO_x) (Zhang et al., 2020), which are usually more concentrated during polluted days in the winter (Sun et al., 2016a). However, the aging process is expected to be slowed in the summer when precursor concentrations are lower. Such an explanation is reasonable and can be supported by the observed thicker coating layer in the winter, as characterized by D_p/D_c (shown in Fig. 8, see Sect. 3.6).

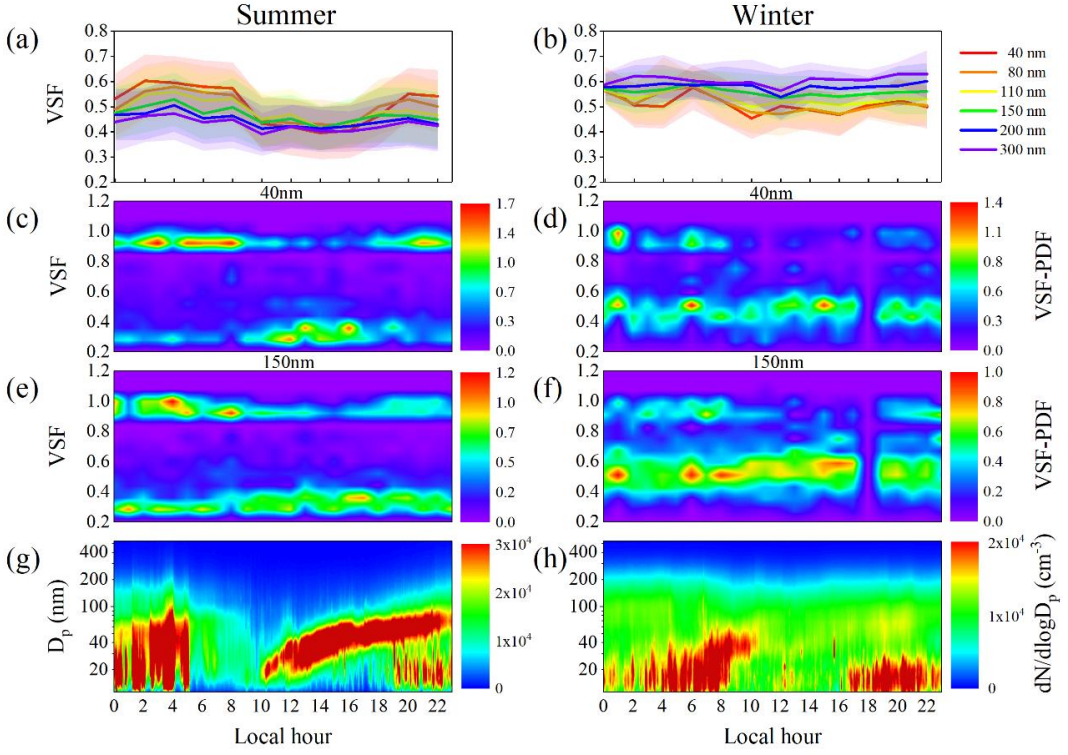

https://doi.org/10.5194/acp-2021-454
Preprint. Discussion started: 5 July 2021


Atmospheric Chemistry and Physics Discussions

Figure 4. Diurnal variation of **(a-b)** mean VSF for all measured dry particle sizes, **(c-f)** mean VSF-PDF for 40- and 150-nm particles, and **(g-h)** mean particle number size distribution during the summer (left) and winter (right) periods. The shade regions in (a-b) denote the standard deviations.

3.4 Number concentrations and fractions of Non-BC, In-BC, and Ex-BC

To study the aerosol mixing state, we retrieved the number concentrations of Non-BC, In-BC, and Ex-BC from the VSF data (Fig. 5). The time series of number concentrations and fractions of 150-nm particles are presented in Figs. 5a and 5b (see Figs. S4 and S5 for the time series of other sizes). Both in the summer and winter cases, large temporal variations in the number concentrations and fractions of Non-BC, In-BC, and Ex-BC were observed, which reflects influences from both local primary urban emissions and addition of secondary species. In the summer, most particles were Non-BC (with mean number fraction of ~67±9 %) because of large contributions from particles formed through nucleation, while In-BC accounted for a small proportion (~23 %). In contrast to the summer case, the majority of particles were In-BC in the winter, with a number fraction of ~55±11 %, reflecting efficient aging and coating of BC particles. Large Non-BC number concentrations and fractions were also observed by Zhang et al. (2017) in the summer at a site in Xianghe (a suburb site close to urban Beijing), where most ambient aerosol particles are Non-BC, with only 7–10 % of particles containing BC. The Ex-BC represents the smallest proportion both in the winter and summer, with number fractions of ~13±10 % and ~10±7 % respectively, suggesting rapid aging and mixing of freshly emitted BC with other species.

https://doi.org/10.5194/acp-2021-454
Preprint. Discussion started: 5 July 2021

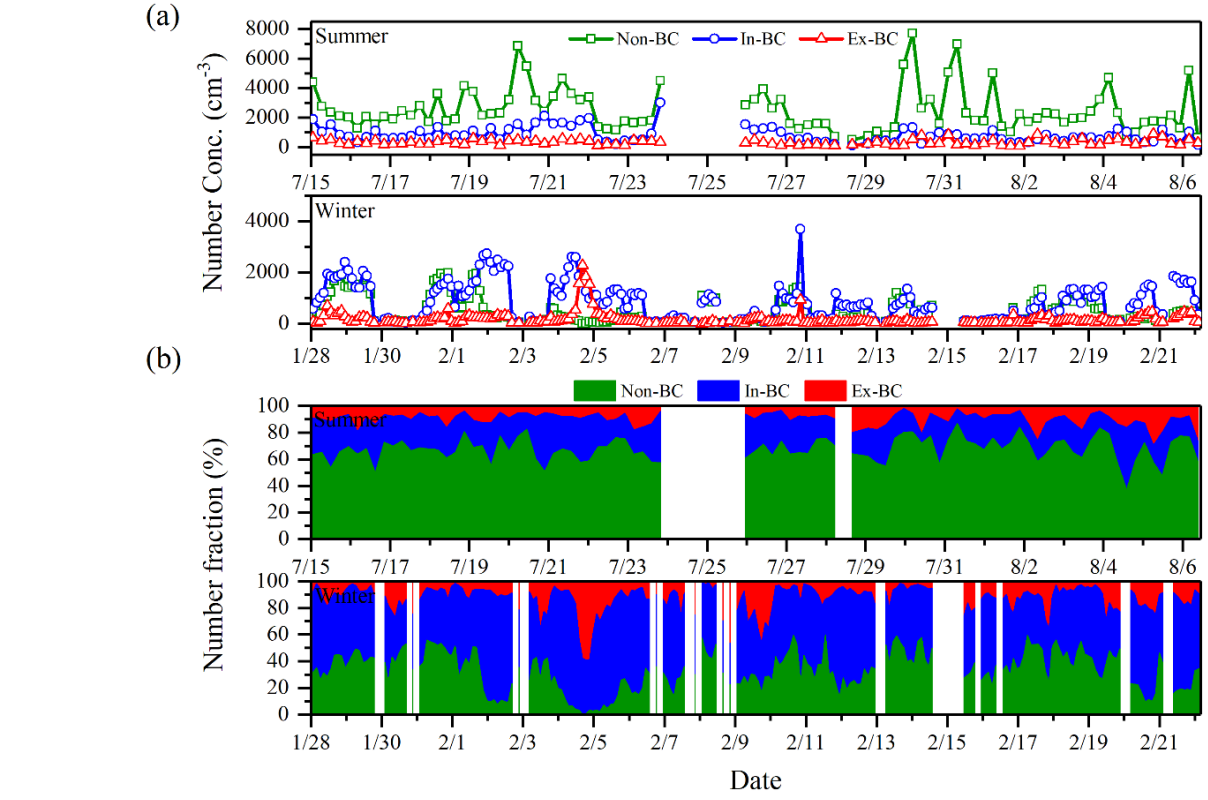

Figure 5. Summer (top) and winter (bottom) time series of **(a)** number concentrations and **(b)** number fractions of Non-BC (in green), In-BC (in blue), and Ex-BC (in red) 150-nm particles.

Figure 6 illustrates the size dependence of the total number fractions of the Non-BC, In-BC, and Ex-BC particles during the summer and winter periods. The number fractions of Non-BC and In-BC are highly size-dependent. In the summer, the number fraction of Non-BC increased with increasing particle size, accounted for 52–69 % of the total number concentration, further demonstrating the large contribution of nucleation to the total concentration of particles and the absence of refractory materials (like BC and charred organics) participating in their growth. While in the winter, the number fraction of In-BC increased and the number fraction of Non-BC decreased with increasing particle size, and BC-containing particles (including Ex-BC and In-BC) dominate and contribute 67–77 % toward the total number concentration, which again suggests that the particles in this size range result from growth of non-volatile primary aerosols (e.g. BC) through addition of more volatile components from coagulation and condensation.

https://doi.org/10.5194/acp-2021-454
Preprint. Discussion started: 5 July 2021

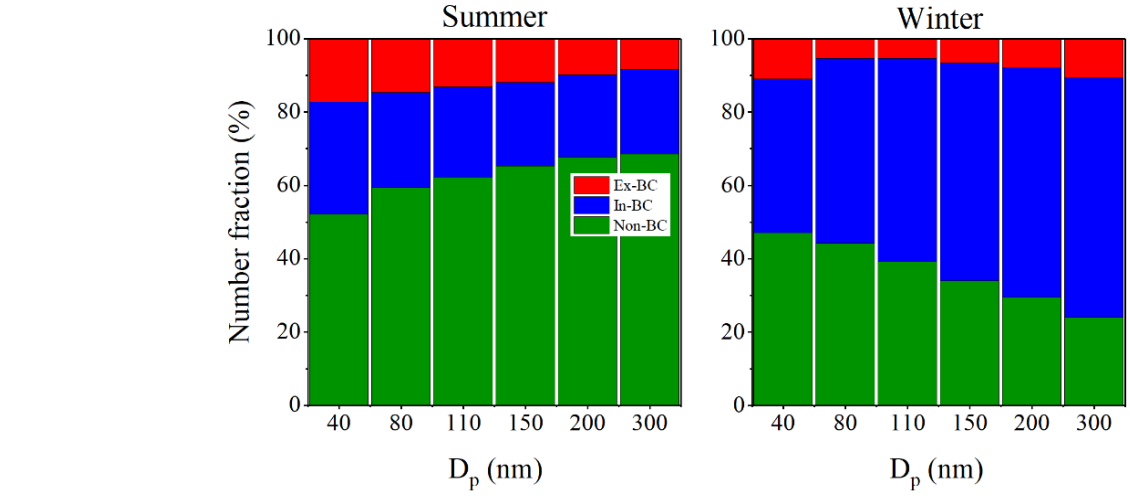

Figure 6. Size-resolved, campaign-averaged number fractions of Non-BC, In-BC, and Ex-BC during the winter (left) and summer (right) periods.

In summary, during the winter most ambient aerosol particles were BC-containing, suggesting that BC particles are a dominant component in urban Beijing. In the summer, however, BC-containing particles contributed much less (only 31–48 %) toward the total number concentration in the measured size range, while Non-BC particles originating from nucleation are the dominant particle type.

3.5 Diurnal variations of retrieved number concentrations and fractions of Non-BC, In-BC, and Ex-BC

Figure 7 shows the diurnal variations of number concentrations and fractions of Non-BC, In-BC and Ex-BC of 40- and 150-nm particles for the summer and winter cases. Diurnal variations are evident for 40 nm and 150 nm Non-BC particles. In the summer, there is a continuous increase in the number concentration and fraction of Non-BC from 10:00 to 14:00 LT, reflecting the impact of new particle formation and growth. The increase concentration/fraction for 150-nm Non-BC particles extended into the late evening (23:00 LT) as particles that nucleated earlier in the day continued to grow into that size range. Compared to the summer, the Non-BC concentration/fraction in the winter exhibits a daily minimum and nightly maximum. This illustrates that the diurnal changes in planetary boundary layer (PBL) dominates the diurnal patterns of Non-BC in cold season when the sources (e.g. nucleation) of Non-BC are insignificant. The diurnal cycles for In-BC are insignificant both in the summer and winter. A slight increase in the number concentration of In-BC is observed during the daytime in the summer

https://doi.org/10.5194/acp-2021-454
Preprint. Discussion started: 5 July 2021


Atmospheric Chemistry and Physics Discussions

for 150-nm particles, likely resulting from rapid photochemical aging that converts the Ex-BC into In-BC particles. However, in the winter, photochemistry and the rate of aging of Ex-BC is reduced, and therefore little or no increase of In-BC around noontime is observed. Instead, its number concentration decreases slightly in the early afternoon (around 14:00 LT) because of the increase in PBL height, resulting in dilution of aged particles with the less polluted air from higher up (Rose et al., 2006). The diurnal variations of number concentrations and fractions of Ex-BC have minima during the daytime and maxima at night for both the summer and winter, consistent with diurnal variations of the PBL height and patterns in urban traffic, which emits fresh Ex-BC particles. These results are in general agreement with previous observations in similar urban environments such as those described by Cheung et al. (2016) and Cheng et al. (2012). In summary, the diurnal variation of aerosol mixing state reflected competition among the processes of photochemical aging, nucleation, local primary emissions, and changes of PBL height. In the summer, photochemical production and growth of particles are the main contributors to Non-BC particles. The rates of aging of BC particles in the urban atmosphere may be similar throughout the day as suggested by the insignificant diurnal variations of In-BC concentration and fraction. In addition to local vehicle emissions and incomplete combustion of fossil fuel, the diurnal variations of Ex-BC concentration are largely impacted by variations of the PBL.

https://doi.org/10.5194/acp-2021-454
Preprint. Discussion started: 5 July 2021

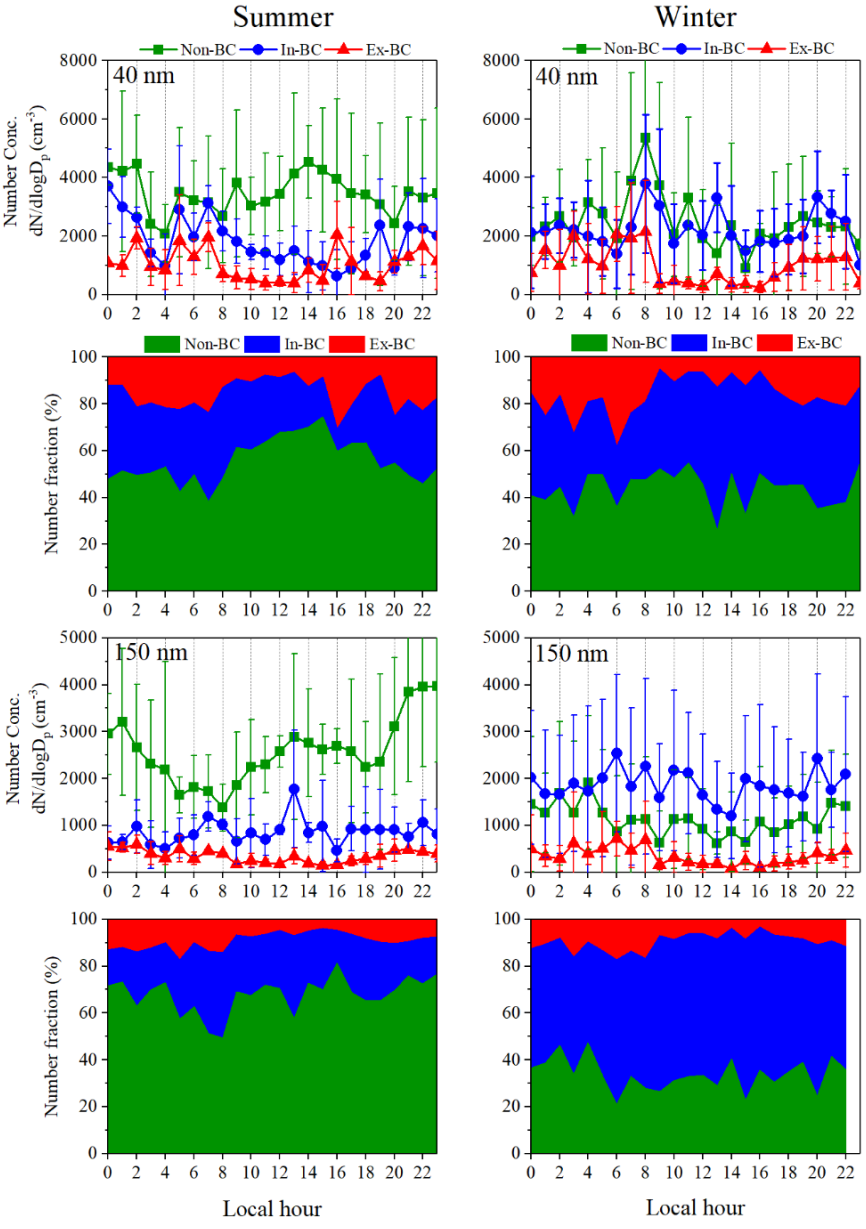

Figure 7. Average diurnal variations of retrieved number concentrations and fractions of Non-BC, In-BC, and Ex-BC of 40- and 150-nm particles in the summer (left) and winter (right) periods.

3.6 Coating thickness characterized by D_p/D_c ratio

The ratio of the BC diameter before and after heating at 300 ℃ (D_p/D_c) was used as a quantitative index to characterize the coating thickness (degree of aging) of BC-containing particles. In the winter,

https://doi.org/10.5194/acp-2021-454
Preprint. Discussion started: 5 July 2021


Atmospheric Chemistry and Physics Discussions

most BC particles have D_p/D_c ratios of 1.6-2.6 (Fig. S6). The large D_p/D_c ratios suggest that the BC particles are thickly coated and likely have a compacted structure following atmospheric aging that results from additional emissions from the residential heating sector and favorable condensation because of the low temperature. While during the summer, the coatings on BC were thinner, with an average D_p/D_c of 1.5 (Fig. 8). In addition, in the winter the D_p/D_c ratio was highly dependent on particle size, with decreasing coating layer thickness with increasing particle size. In the summer, it was independent of particle size.

Our results are similar to those reported previously in similar urban environments (Wehner et al., 2004; Zhang et al., 2018; Liu et al., 2019). For example, Liu et al. (2019) found BC coating thickness was more variable in the winter than in the summer, and that the average coating thickness on BC particles was higher in the winter. Zhang et al. (2018) showed that the size-dependence of the D_p/D_c ratio was associated with air pollution and indicated that the aging of smaller BC cores was more sensitive to air pollution levels.

Previous modelling studies have reported that coating materials on BC particles can significantly enhance the light absorption of BC via the lensing effect (Jacobson, 2001; Moffet and Prather, 2009; Lack and Cappa, 2010; Zhang et al., 2020). Thus, aging of BC-containing particles enhances their light absorption efficiency. However, how the aging and light absorption capability of BC particles will change under different ambient conditions remains unclear. The differences in coating thickness on BC particles we observed between summer and winter can help to parametrize the BC absorption enhancement in models.

https://doi.org/10.5194/acp-2021-454
Preprint. Discussion started: 5 July 2021

Atmospheric Chemistry and Physics Discussions

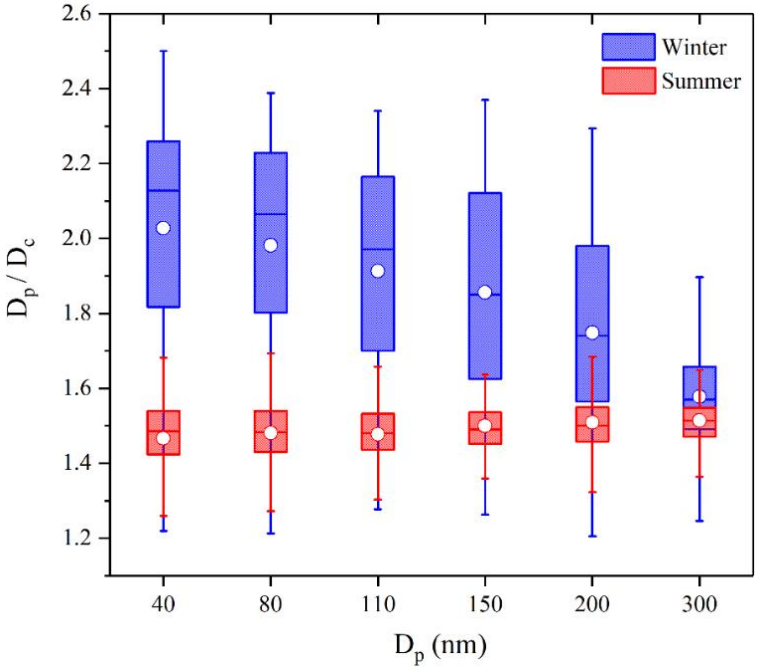

Figure 8. Size-dependent mean D_p/D_c ratio (circular markers) of fine aerosol particles during the winter (in blue) and summer (in red) periods. The boxes show the 25th, 50th, and 75th percentiles. The extremities show the 5th and 95th percentiles.

4 Conclusion

In this study, the volatility of the fine particles is characterized as VSF and the results from wintertime and summertime are shown and compared. Results show that the measured VSF-PDF is almost always bimodal, with one high-volatile and one less- or non-volatile mode, both in the summer and winter. The mean VSF-PDF has a pronounced HV mode in the summer, generally with a VSF minimum at ~0.2, while in the winter a broad MV mode spans much of the measured VSF range (with VSF minimum at 0.45-0.65), reflecting lower average volatility in the winter. Diurnal variations in VSF of 40-nm particles are evident only in the summer, with a prominent HV mode resulting from new particle formation and growth present around noontime and early afternoon and a dominant LV mode during nighttime. No such feature is evident in the winter measurements.

The mixing state of ambient fine particles was calculated from the size-resolved VSF and the results for summer and winter compared and contrasted. On average, black carbon (BC)-containing

https://doi.org/10.5194/acp-2021-454
Preprint. Discussion started: 5 July 2021


Atmospheric Chemistry and Physics Discussions

particles contributed 67–77 % toward the total number concentration in the winter, indicating that BC particles are a dominant component of the wintertime Beijing aerosol. In the summer, nucleation and particle growth results in a dominant population of volatile, Non-BC, particles, which account for 52–69 % of the total concentration in the measured size range. The diurnal cycles of the retrieved particle mixing state in the summer further show that rapid photochemical processing and nucleation are the main contributors to Non-BC particles. The rates of aging of BC in this and similar urban environments may be relatively constant through the day as indicated by the minimal diurnal variations of In-BC concentration and fraction. In addition to local vehicle emissions and other fossil fuel combustion, the diurnal variations of Ex-BC are largely impacted by the variations of PBL. Finally, we also report on the degree of aging, as characterized by the ratio of the BC particle diameter before and after heating at 300 ℃ (D_p/D_c), with an average of ~2.2 in the winter and ~1.5 in the summer. The results indicate BC particles are more thickly coated in wintertime. Our results could help elucidate the effects of particle growth mechanisms on volatility and mixing state during cold and warm seasons in polluted urban areas such as Beijing.

Data availability. All data needed to evaluate the conclusions in the paper are present in the paper and/or the Supplementary Materials. Also, all data used in the study are available from the corresponding author upon request (fang.zhang@bnu.edu.cn).

Author contributions. F. Z. and L. C. conceived the conceptual development of the manuscript. L. C. directed and performed of the experiments with J. L., S. J., J. R., and F. Z. and L. C. conducted the data analysis and wrote the draft of the manuscript, and all authors edited and commented on the various sections of the manuscript.

Declaration of competing interest. The authors declare no competing interests.

Acknowledgments. This work was funded by NSFC research projects (41975174, 41675141), and the National Basic Research Program of China (2017YFC1501702). We thank all participants in the field campaigns for their tireless work and cooperation.

https://doi.org/10.5194/acp-2021-454
Preprint. Discussion started: 5 July 2021

Atmospheric Chemistry and Physics Discussions

References

Baklanov, A., Molina, L. T., and Gauss, M.: Megacities, air quality and climate, Atmospheric Environment, 126, 235-249, https://doi.org/10.1016/j.atmosenv.2015.11.059, 2016.

Bidleman, T. F.: Atmospheric processes, Environmental Science & Technology, 22, 361-367, 10.1021/es00169a002, 1988.

Brooks, B. J., Smith, M. H., Hill, M. K., and O'Dowd, C. D.: Size-differentiated volatility analysis of internally mixed laboratory-generated aerosol, Journal of Aerosol Science, 33, 555-579, https://doi.org/10.1016/S0021-8502(01)00192-6, 2002.

Cai, M., Tan, H., Chan, C. K., Mochida, M., Hatakeyama, S., Kondo, Y., Schurman, M. I., Xu, H., Li, F., Shimada, K., Li, L., Deng, Y., Yai, H., Matsuki, A., Qin, Y., and Zhao, J.: Comparison of Aerosol Hygroscopcity, Volatility, and Chemical Composition between a Suburban Site in the Pearl River Delta Region and a Marine Site in Okinawa, Aerosol and Air Quality Research, 17, 3194-3208, 10.4209/aaqr.2017.01.0020, 2017.

Cappa, C. D., Onasch, T. B., Massoli, P., Worsnop, D. R., Bates, T. S., Cross, E. S., Davidovits, P., Hakala, J., Hayden, K. L., Jobson, B. T., Kolesar, K. R., Lack, D. A., Lerner, B. M., Li, S.-M., Mellon, D., Nuaaman, I., Olfert, J. S., Petäjä, T., Quinn, P. K., Song, C., Subramanian, R., Williams, E. J., and Zaveri, R. A.: Radiative Absorption Enhancements Due to the Mixing State of Atmospheric Black Carbon, Science, 337, 1078, 10.1126/science.1223447, 2012.

Chen, L., Zhang, F., Yan, P., Wang, X., Sun, L., Li, Y., Zhang, X., Sun, Y., and Li, Z.: The large proportion of black carbon (BC)-containing aerosols in the urban atmosphere, Environmental Pollution, 263, 114507, https://doi.org/10.1016/j.envpol.2020.114507, 2020.

Chen, S.-C., Tsai, C.-J., Huang, C.-Y., Chen, H.-D., Chen, S.-J., Lin, C.-C., Tsai, J.-H., Chou, C. C. K., Lung, S. C. C., Huang, W.-R., Roam, G.-D., Wu, W.-Y., Smolik, J., and Dzumbova, L.: Chemical Mass Closure and Chemical Characteristics of Ambient Ultrafine Particles and other PM Fractions, Aerosol Science and Technology, 44, 713-723, 10.1080/02786826.2010.486385, 2010.

Cheng, Y. F., Berghof, M., Garland, R. M., Wiedensohler, A., Wehner, B., Müller, T., Su, H., Zhang, Y. H., Achtert, P., Nowak, A., Pöschl, U., Zhu, T., Hu, M., and Zeng, L. M.: Influence of soot mixing

https://doi.org/10.5194/acp-2021-454
Preprint. Discussion started: 5 July 2021

state on aerosol light absorption and single scattering albedo during air mass aging at a polluted regional site in northeastern China, 114, 10.1029/2008jd010883, 2009.

Cheng, Y. F., Su, H., Rose, D., Gunthe, S. S., Berghof, M., Wehner, B., Achtert, P., Nowak, A., Takegawa, N., Kondo, Y., Shiraiwa, M., Gong, Y. G., Shao, M., Hu, M., Zhu, T., Zhang, Y. H., Carmichael, G. R., Wiedensohler, A., Andreae, M. O., and Pöschl, U.: Size-resolved measurement of the mixing state of soot in the megacity Beijing, China: diurnal cycle, aging and parameterization, Atmos. Chem. Phys., 12, 4477-4491, 10.5194/acp-12-4477-2012, 2012.

Cheung, H. H. Y., Tan, H., Xu, H., Li, F., Wu, C., Yu, J. Z., and Chan, C. K.: Measurements of non-volatile aerosols with a VTDMA and their correlations with carbonaceous aerosols in Guangzhou, China, Atmos. Chem. Phys., 16, 8431-8446, 10.5194/acp-16-8431-2016, 2016.

Dzubay, T. G., Stevens, R. K., Lewis, C. W., Hern, D. H., Courtney, W. J., Tesch, J. W., and Mason, M. A.: Visibility and aerosol composition in Houston, Texas, Environmental Science & Technology, 16, 514-525, 10.1021/es00102a017, 1982.

Frey, A., Rose, D., Wehner, B., Müller, T., Cheng, Y., Wiedensohler, A., and Virkkula, A.: Application of the Volatility-TDMA Technique to Determine the Number Size Distribution and Mass Concentration of Less Volatile Particles, Aerosol Science and Technology, 42, 817-828, 10.1080/02786820802339595, 2008.

Gao, Y., Liu, X., Zhao, C., and Zhang, M.: Emission controls versus meteorological conditions in determining aerosol concentrations in Beijing during the 2008 Olympic Games, Atmos. Chem. Phys., 11, 12437-12451, 10.5194/acp-11-12437-2011, 2011.

Glasius, M., and Goldstein, A. H.: Recent Discoveries and Future Challenges in Atmospheric Organic Chemistry, Environmental Science & Technology, 50, 2754-2764, 10.1021/acs.est.5b05105, 2016.

Grieshop, A. P., Lipsky, E. M., Pekney, N. J., Takahama, S., and Robinson, A. L.: Fine particle emission factors from vehicles in a highway tunnel: Effects of fleet composition and season, Atmospheric Environment, 40, 287-298, https://doi.org/10.1016/j.atmosenv.2006.03.064, 2006.

Gysel, M., McFiggans, G. B., and Coe, H.: Inversion of tandem differential mobility analyser (TDMA) measurements, Journal of Aerosol Science, 40, 134-151, https://doi.org/10.1016/j.jaerosci.2008.07.013, 2009.

https://doi.org/10.5194/acp-2021-454
Preprint. Discussion started: 5 July 2021


Atmospheric Chemistry and Physics Discussions

Huffman, J. A., Docherty, K. S., Aiken, A. C., Cubison, M. J., Ulbrich, I. M., DeCarlo, P. F., Sueper, D., Jayne, J. T., Worsnop, D. R., Ziemann, P. J., and Jimenez, J. L.: Chemically-resolved aerosol volatility measurements from two megacity field studies, Atmos. Chem. Phys., 9, 7161-7182, 10.5194/acp-9-7161-2009, 2009.

Jacobson, M. Z.: Strong radiative heating due to the mixing state of black carbon in atmospheric aerosols, Nature, 409, 695-697, 10.1038/35055518, 2001.

Jiang, S., Ye, X., Wang, R., Tao, Y., Ma, Z., Yang, X., and Chen, J.: Measurements of nonvolatile size distribution and its link to traffic soot in urban Shanghai, Science of The Total Environment, 615, 452-461, https://doi.org/10.1016/j.scitotenv.2017.09.176, 2018.

Kuhn, T., Krudysz, M., Zhu, Y., Fine, P. M., Hinds, W. C., Froines, J., and Sioutas, C.: Volatility of indoor and outdoor ultrafine particulate matter near a freeway, Journal of Aerosol Science, 36, 291-302, https://doi.org/10.1016/j.jaerosci.2004.09.006, 2005.

Lack, D. A., and Cappa, C. D.: Impact of brown and clear carbon on light absorption enhancement, single scatter albedo and absorption wavelength dependence of black carbon, Atmos. Chem. Phys., 10, 4207-4220, 10.5194/acp-10-4207-2010, 2010.

Levy, M. E., Zhang, R., Zheng, J., Tan, H., Wang, Y., Molina, L. T., Takahama, S., Russell, L. M., and Li, G.: Measurements of submicron aerosols at the California–Mexico border during the Cal–Mex 2010 field campaign, Atmospheric Environment, 88, 308-319, https://doi.org/10.1016/j.atmosenv.2013.08.062, 2014.

Liu, D., Joshi, R., Wang, J., Yu, C., Allan, J. D., Coe, H., Flynn, M. J., Xie, C., Lee, J., Squires, F., Kotthaus, S., Grimmond, S., Ge, X., Sun, Y., and Fu, P.: Contrasting physical properties of black carbon in urban Beijing between winter and summer, Atmos. Chem. Phys., 19, 6749-6769, 10.5194/acp-19-6749-2019, 2019.

Meyer, M. B., Patashnick, H., Ambs, J. L., and Rupprecht, E.: Development of a sample equilibration system for the TEOM continuous PM monitor, Journal of the Air & Waste Management Association (1995), 50, 1345-1349, 10.1080/10473289.2000.10464180, 2000.

https://doi.org/10.5194/acp-2021-454
Preprint. Discussion started: 5 July 2021

Moffet, R. C., and Prather, K. A.: In-situ measurements of the mixing state and optical properties of soot with implications for radiative forcing estimates, Proceedings of the National Academy of Sciences, 106, 11872, 10.1073/pnas.0900040106, 2009.

Nordmann, S., Cheng, Y. F., Carmichael, G. R., Yu, M., Denier van der Gon, H. A. C., Zhang, Q., Saide, P. E., Pöschl, U., Su, H., Birmili, W., and Wiedensohler, A.: Atmospheric black carbon and warming effects influenced by the source and absorption enhancement in central Europe, Atmos. Chem. Phys., 14, 12683-12699, 10.5194/acp-14-12683-2014, 2014.

Philippin, S., Wiedensohler, A., and Stratmann, F.: Measurements of non-volatile fractions of pollution aerosols with an eight-tube volatility tandem differential mobility analyzer (VTDMA-8), Journal of Aerosol Science, 35, 185-203, https://doi.org/10.1016/j.jaerosci.2003.07.004, 2004.

Pöschl, U.: Atmospheric Aerosols: Composition, Transformation, Climate and Health Effects, 44, 7520-7540, 10.1002/anie.200501122, 2005.

Rose, D., Wehner, B., Ketzel, M., Engler, C., Voigtländer, J., Tuch, T., and Wiedensohler, A.: Atmospheric number size distributions of soot particles and estimation of emission factors, Atmos. Chem. Phys., 6, 1021-1031, 10.5194/acp-6-1021-2006, 2006.

Saha, P. K., Khlystov, A., and Grieshop, A. P.: Downwind evolution of the volatility and mixing state of near-road aerosols near a US interstate highway, Atmos. Chem. Phys., 18, 2139-2154, 10.5194/acp-18-2139-2018, 2018.

Sakurai, H., Park, K., McMurry, P. H., Zarling, D. D., Kittelson, D. B., and Ziemann, P. J.: Size-Dependent Mixing Characteristics of Volatile and Nonvolatile Components in Diesel Exhaust Aerosols, Environmental Science & Technology, 37, 5487-5495, 10.1021/es034362t, 2003.

Sun, Y., Chen, C., Zhang, Y., Xu, W., Zhou, L., Cheng, X., Zheng, H., Ji, D., Li, J., Tang, X., Fu, P., and Wang, Z.: Rapid formation and evolution of an extreme haze episode in Northern China during winter 2015, Scientific Reports, 6, 27151, 10.1038/srep27151, 2016a.

Sun, Y., Wang, Z., Wild, O., Xu, W., Chen, C., Fu, P., Du, W., Zhou, L., Zhang, Q., Han, T., Wang, Q., Pan, X., Zheng, H., Li, J., Guo, X., Liu, J., and Worsnop, D. R.: "APEC Blue": Secondary Aerosol Reductions from Emission Controls in Beijing, Scientific Reports, 6, 20668, 10.1038/srep20668, 2016b.

https://doi.org/10.5194/acp-2021-454
Preprint. Discussion started: 5 July 2021


Atmospheric Chemistry and Physics Discussions

Villani, P., Picard, D., Marchand*, N., and Laj, P.: Design and Validation of a 6-Volatility Tandem Differential Mobility Analyzer (VTDMA), Aerosol Science and Technology, 41, 898-906, 10.1080/02786820701534593, 2007.

Wang, T., Nie, W., Gao, J., Xue, L. K., Gao, X. M., Wang, X. F., Qiu, J., Poon, C. N., Meinardi, S., Blake, D., Wang, S. L., Ding, A. J., Chai, F. H., Zhang, Q. Z., and Wang, W. X.: Air quality during the 2008 Beijing Olympics: secondary pollutants and regional impact, Atmos. Chem. Phys., 10, 7603-7615, 10.5194/acp-10-7603-2010, 2010.

Wang, Y., Zhang, F., Li, Z., Tan, H., Xu, H., Ren, J., Zhao, J., Du, W., and Sun, Y.: Enhanced hydrophobicity and volatility of submicron aerosols under severe emission control conditions in Beijing, Atmos. Chem. Phys., 17, 5239-5251, 10.5194/acp-17-5239-2017, 2017.

Wehner, B., Philippin, S., Wiedensohler, A., Scheer, V., and Vogt, R.: Variability of non-volatile fractions of atmospheric aerosol particles with traffic influence, Atmospheric Environment, 38, 6081-6090, https://doi.org/10.1016/j.atmosenv.2004.08.015, 2004.

Wehner, B., Berghof, M., Cheng, Y. F., Achtert, P., Birmili, W., Nowak, A., Wiedensohler, A., Garland, R. M., Pöschl, U., Hu, M., and Zhu, T.: Mixing state of nonvolatile aerosol particle fractions and comparison with light absorption in the polluted Beijing region, 114, 10.1029/2008jd010923, 2009.

Yeung, M. C., Lee, B. P., Li, Y. J., and Chan, C. K.: Simultaneous HTDMA and HR-ToF-AMS measurements at the HKUST Supersite in Hong Kong in 2011, Journal of Geophysical Research: Atmospheres, 119, 9864-9883, 10.1002/2013JD021146, 2014.

Zhang, F., Wang, Y., Peng, J., Chen, L., Sun, Y., Duan, L., Ge, X., Li, Y., Zhao, J., Liu, C., Zhang, X., Zhang, G., Pan, Y., Wang, Y., Zhang, A. L., Ji, Y., Wang, G., Hu, M., Molina, M. J., and Zhang, R.: An unexpected catalyst dominates formation and radiative forcing of regional haze, Proceedings of the National Academy of Sciences, 117, 3960, 10.1073/pnas.1919343117, 2020.

Zhang, S. L., Ma, N., Kecorius, S., Wang, P. C., Hu, M., Wang, Z. B., Größ, J., Wu, Z. J., and Wiedensohler, A.: Mixing state of atmospheric particles over the North China Plain, Atmospheric Environment, 125, 152-164, https://doi.org/10.1016/j.atmosenv.2015.10.053, 2016.

Zhang, Y., Su, H., Kecorius, S., Wang, Z., Hu, M., Zhu, T., He, K., Wiedensohler, A., Zhang, Q., and Cheng, Y.: Mixing State of Refractory Black Carbon of the North China Plain Regional Aerosol

https://doi.org/10.5194/acp-2021-454
Preprint. Discussion started: 5 July 2021

Atmospheric Chemistry and Physics Discussions

Combining a Single Particle Soot Photometer and a Volatility Tandem Differential Mobility Analyzer, Atmos. Chem. Phys. Discuss., 2017, 1-27, 10.5194/acp-2017-222, 2017.

Zhang, Y., Zhang, Q., Cheng, Y., Su, H., Li, H., Li, M., Zhang, X., Ding, A., and He, K.: Amplification of light absorption of black carbon associated with air pollution, Atmos. Chem. Phys., 18, 9879-9896, 10.5194/acp-18-9879-2018, 2018.